Desalination and Water Treatment
www.deswater.com

doi:10.5004/dwt.2017.0064

61 (2017) 1–11
January

Effect of membrane fouling on wetting in membrane distillation system

Yonghyun Shin, Yongjun Choi, Jihyuck Choi, Yongsun Jang, Sangho Lee*

School of Civil and Environmental Engineering, Kookmin University, Jeongneung-gil 77, Seongbuk-gu, Seoul 136-702, Korea, Tel. +82 2 910 4529, Fax +82 2 910 4939, email: sanghlee@kookmin.ac.kr

Received 17 January 2016; Accepted 2 August 2016

ABSTRACT

Although membrane distillation (MD) has attracted significant attention as a promising technology for seawater desalination and wastewater reuse, membrane fouling and pore wetting are two major problems to be overcome prior to its widespread application. In this study, a series of MD experiments were carried out to investigate the effect of foulant characteristics on fouling and wetting of MD membranes. The interactions among different foulants and their impact on fouling and wetting were also examined. Synthetic feed solutions were prepared using model foulants including alginate, $CaCO_3$, and colloidal silica. Water flux and liquid entry pressure (LEP) were simultaneously monitored to quantify the extents of fouling and wetting. Results showed that fouling propensities of single foulant and the mixtures of different foulants were quite different, suggesting the "positive" and "negative" synergic effects of multiple foulants. Pore wetting was not observed in the treatment of feed solutions containing single foulant. However, a combination of different foulants led to reduction in LEP, indicating the occurrence of pore wetting by the synergic effect of multiple foulants.

Keywords: Membrane distillation; Fouling; Wetting; LEP (Liquid entry pressure)

1. Introduction

Access to clean water supply continues to be the most urgent and pressing global issue where economic and ecological needs have urged for more water-efficient technologies [1]. In this context, desalination has become imperative as a drinking water source to meet the water demands in many water-scarce regions [2,3]. Desalination technologies have evolved and advanced rapidly along with increasing water demands around the world since 1950s [3]. Among many desalination technologies, reverse osmosis (RO) is playing an increasingly important role to provide sufficient water resources of desirable quality for a wide spectrum of applications [1,4]. Nevertheless, RO desalination is still limited due primarily to high energy requirements which are currently met with expensive fossil fuels [5].

Accordingly, desalination powered by renewable energy sources is becoming an attractive solution to address the issues related to high electricity consumption [5–7]. A promising technology for renewable energy desalination is membrane distillation (MD), which may be paired with low-grade heat such as solar thermal energy, geothermal energy, and waste heat [1,2,7,8]. MD is a thermal process driven by the difference in vapor pressure between feed water and distillate (product water) [5,6]. Unlike RO, MD uses hydrophobic microporous membranes that act as barriers to separate vapor from liquid water [8–10]. Potential application of MD includes not only renewable-energy desalination but also decentralized potable water treatment [11,12], food processing [13,14], and zero liquid discharge [15].

Nevertheless, one principal challenge for MD is fouling and pore wetting of the MD membrane [16–19]. As feed water contains a variety of impurities such as salts, organic matters, colloids, and suspended particles, the membrane in MD process may experience irreversible attachment of these compounds. Moreover, MD membranes are mostly hydrophobic, leading to strong interactions with hydrophobic chemicals in the feed water [19]. Crystallization of sparingly soluble ions

*Corresponding author.

Presented at the 8th International Conference on Challenges in Environmental Science & Engineering (CESE-2015), 28 September–2 October 2015, Sydney, Australia.

including $CaCO_3$, $CaSO_4$, and silica may also result in severe fouling [17]. Pore wetting, which is defined as penetration of water into membrane pores, is another serious problem in MD process because it reduces solute rejection [20]. In addition, wetting may occur together with fouling [19].

Many studies have focused on fouling phenomena and wetting behaviors in MD process and emphasized the importance of their fundamental understanding [9,10,16–20]. Despite these efforts, these studies mainly focused on MD fouling caused by single component such as scale-forming ions [21,22], organic matters [23], and silica [24]. Interactions among different foulants, although they seem to be important, have not revealed yet in MD process. In addition, the relationship between fouling and wetting has not been sufficiently studied. Accordingly, the objectives of this work are to examine fouling propensity of various model foulants and to estimate the impact of fouling on wetting in MD process. Synergy effect of different foulants on MD performance was also investigated.

2. Experimental procedure

2.1. MD membrane and experimental setup

Commercially available flat sheet membranes (Millipore, USA) made of PVDF (polyvinylidene fluoride) were used. The nominal pore size of the membranes was 0.22 μm. The contact angle was measured to be 120°. The membrane was placed on a pre-fabricated plate-and-frame module that has the effective membrane area of 12 cm^2.

The experiments were performed in direct contact MD (DCMD) mode using a test equipment as shown in Fig. 1. Up to six MD modules could be simultaneously used in this equipment. The working temperatures for feed and distillate were controlled by heaters and by a water bath. The stirring speed was controlled by a magnetic stirrer plate. The temperatures of the feed solution and the distillate were adjusted to 60°C and 20°C, respectively. The flow rates of the feed solution and the distillate were adjusted to 700 and 500 mL min^{-1}, respectively. An electronic balance connected to a data logger was used to continuously measure water flux through the membrane. Each experiment was performed over 2,000 min, and the change in membrane permeability was expressed as the ratio of final flux (J_f) to initial flux (J_i).

Table 1
Summary of experimental conditions

Operation type	DCMD (direct contact membrane distillation)
Membrane type	PVDF flat sheet membrane (Millipore)
Flow rate	Feed side: 0.7 L min^{-1}
	distillate side: 0.4 L min^{-1}
Temperature	Feed side: 60°C
	distillate side: 20°C

2.2. Feed solutions

Total eleven solutions were used as synthetic feed waters to the MD system, as shown in Table 2. Model foulants including alginate, $CaCO_3$, and colloidal silica nanoparticles (Ludox SM and Ludox TMA) were added to deionized water to prepare these feed solutions. Not only single foulant solutions (AL, CA, SM, TMA) but also

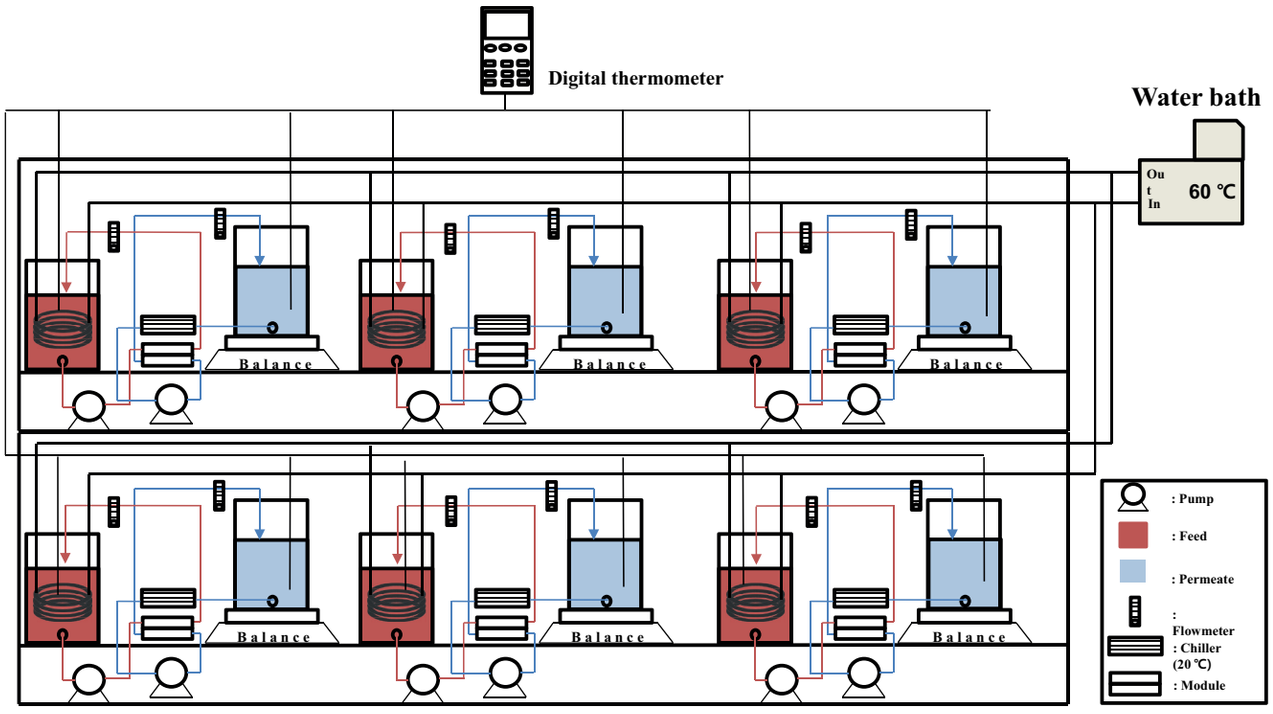

Fig. 1. Schematic diagram of direct contact membrane distillation (DCMD) system.

Table 2
Summary of feed solutions

Notation	Foulant(s)
AL	Alginate 500 mg L^{-1}
CA	$CaCO_3$ 100 mg L^{-1}
SM	Ludox SM 500 mg L^{-1}
TMA	Ludox TMA 500 mg L^{-1}
AL+SM	Alginate 500 mg L^{-1} + Ludox SM 500 mg L^{-1}
AL+TMA	Alginate 500 mg L^{-1} + Ludox TMA 500 mg L^{-1}
CA+SM	$CaCO_3$ 100 mg L^{-1} + Ludox SM 500 mg L^{-1}
CA+TMA	$CaCO_3$ 100 mg L^{-1} + Ludox TMA 500 mg L^{-1}
AL+CA	Alginate 500 mg L^{-1} + $CaCO_3$ 100 mg L^{-1}
AL+CA+SM	Alginate 500 mg L^{-1} + $CaCO_3$ 100 mg L^{-1}+ Ludox SM 500 mg L^{-1}
AL+CA+TMA	Alginate 500 mg L^{-1} + $CaCO_3$ 100 mg L^{-1} + Ludox TMA 500 mg L^{-1}

binary (AL+SM, AL+TMA, CA+SM, CA+TMA, AL+CA) and tertiary (AL+CA+SM, AL+CA+TMA) foulant solutions were employed. Two colloidal silica particles (SM and TMA) with different sizes were selected as the model foulants to investigate the effect of colloid size on fouling propensity. According to the manufacturer, the sizes of Ludox SM and TMA were 7 and 22 nm, respectively. The foulant concentrations were chosen to accelerate fouling in MD experiments. Accordingly, the foulant concentrations were higher than those in normal conditions.

2.3. Liquid entry pressure

The liquid entry pressure (LEP) is an imperative property of MD membranes since it represents the pressure over which liquid water can enter the membrane pores. Once the pores are filled with water, solutes may directly pass through the membrane, thereby affecting the quality of the product water. Accordingly, the operating pressure should not be higher than LEP of the MD membrane. LEP is also an index for the tendency of membrane wetting because membranes with lower LEP is susceptible to wetting.

There are several factors affecting the LEP of the membrane. If the membrane is strongly hydrophobic and has relatively small pores, its LEP value is high. Such relationship can be theoretically described by the Laplace (Cantor) equation:

$$\mathrm{LEP} = \frac{-2B\gamma\cos(\theta)}{r_{\max}}$$

where B is a geometric factor for which a value of 1 indicates circular pores; γ is the liquid surface tension; θ is the liquid–solid contact angle; and r_{max} is the largest pore radius.

In this study, the LEP of the membranes were directly measured using a device illustrated in Fig. 2. The system consists of a high-pressure nitrogen cylinder, a pressure regulator, a pressure vessel, a pressure gauge, and a membrane holder. The applied pressure increased stepwise before the penetration of water through the membrane was observed. The measurements were triplicated to obtain reliable results.

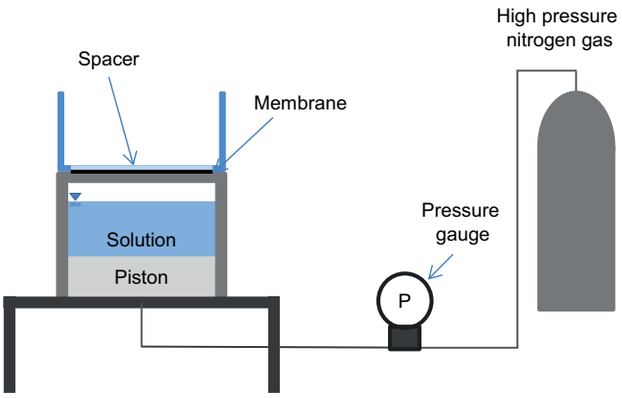

Fig. 2. Schematic diagram of liquid entry pressure (LEP) measurement device.

2.4. Scanning electron microscope

A field-enhanced scanning electron microscopy (SEM; Hitachi S-4700) was used to identify morphology of fouling layer or foulant deposit on membrane surface. Since the morphology of foulants is different, SEM image could be used to identify the foulant. Prior to the SEM analysis, MD membranes were dried at a room temperature and coated by platinum. The thickness of the platinum coating ranged from 2 to 10 nm.

3. Results and discussion

3.1. Fouling caused by single foulant solutions

In order to examine the effect of single foulant on MD performance, flux measurements were carried out for the feed solutions including AL (alginate only), CA ($CaCO_3$ only), SM (Ludox SM only), and TMA (Ludox TMA only) under the following operating conditions: feed temperature, 60°C; distillate temperature, 20°C; and the initial flux, 11.5 kg m^{-2}-h^{-1}. The results are shown in Fig. 3. After the MD operation of 2,250 min, the final flux values for AL, CA, SM, and TMA were 95.6%, 85.6%, 87.1%, and 87.9%, respectively, of the initial flux. This suggests that the fouling propensities for these single foulants are not sufficiently high to cause rapid flux decline. Nevertheless, $CaCO_3$ showed the highest fouling potential among these four model foulants. It appears that the deposition of $CaCO_3$ particles as well as scale formation on the membrane surface may result in moderate fouling.

The SEM images of the MD membranes before and after the fouling tests are shown in Fig. 4. The magnification ratio was 5000 in all cases. In case of AL and TMA, the surfaces of the membrane were not covered by foulants and look similar to that of new membrane. On the other hand, the deposition of foulant could be observed in the case of CA and SM. In fact, this order of surface coverage by foulant is inversely reflected in the order of final water fluxes in Fig. 3. The higher deposition of foulant for Ludox SM than Ludox TMA is attributed to their size difference. Since the Ludox SM is smaller (7 nm) than the Ludox TMA (22 nm), it is easier to deposit on the membrane surface. In summary, it is evident from the results in Figs. 3 and 4 that the fouling

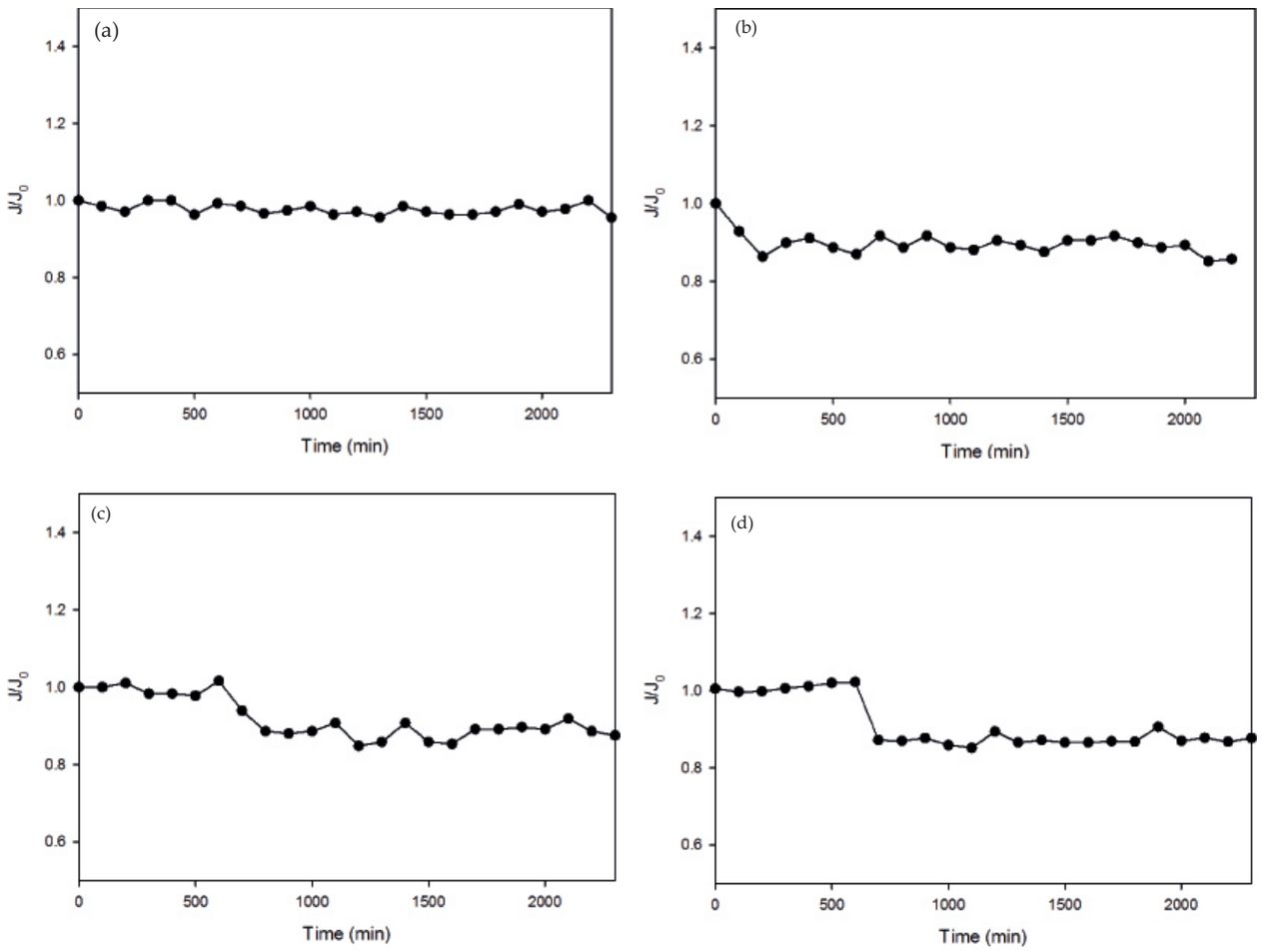

Fig. 3. Flux decline for membrane distillation (MD) of single foulant solutions: (a) AL (Alginate, 500 mg L^{-1}), (b) CA ($CaCO_3$, 100 mg L^{-1}), (c) SM (Ludox SM, 500 mg L^{-1}), and (d) TMA (Ludox TMA, 500 mg L^{-1}).

potentials for single foulant solutions were not substantial except for CA.

3.2. Fouling caused by binary foulant solutions

In addition to the fouling experiments using the single foulant solutions, a series of experiments were carried out using the binary foulant solutions listed in Table 2. The results for AL+SM and AL+TMA are shown in Fig. 5. The permeate flux for these binary foulant solutions was significantly reduced compared with the permeate flux for the single foulant solutions: AL, SM, and TMA. The J/J_0 values for AL and SM were 0.956 and 0.871, respectively. In other words, 1-J/J_0 values for AL and SM are 0.044 and 0.129, respectively. If these foulants individually caused flux decline, 1-J/J_0 value for AL+SM should be the sum of two values (0.044+0.129 = 0.173), and thus J/J_0 for AL+SM should be 0.827. However, the J/J_0 for AL+SM determined from the experiment is 0.871 as shown in Fig. 5(a). The additional reduction in J/J_0 by 0.097 seems to result from synergic effect by combination of alginate and Ludox SM nanoparticles. Similarly, the J/J_0 value for AL+SM was only 0.767 while those for AL and SM were 0.956 and 0.879, respectively. In this case, the synergic effect seems to reduce the J/J_0 value by 0.68.

The SEM images in Fig. 6 also confirmed the synergic effect in the binary foulant solutions. As shown in Figs. 4(b) and 4(d), alginate and Ludox SM resulted in moderate fouling. Membrane pores could be found even after membrane fouling in both cases. Compared with these cases, the binary foulant solution containing alginate and SM led to more severe fouling as indicated by the Fig. 6(a). The membrane was fully covered, and the foulant layer appears to be thicker. Similar tendency was found from alginate and Ludox TMA as shown in Figs. 4(b), 4(e), and 6(b). This suggests that the deposition of the foulants was accelerated by the synergic effect. It seems that the alginate and silica nanoparticles form floc-like structures that are easy to form deposits on the membrane surface. The additional flux decline shown in Fig. 5 can also be explained by this mechanism.

Fig. 7 shows the decline in flux for the CA+AL foulant solution. In this case, the J/J_0 value was 0.910, which is lower than that for CA and larger than that for AL. Unlike the case of alginate and silica nanoparticles, the accelerated fouling by the synergic effect of binary foulants did not

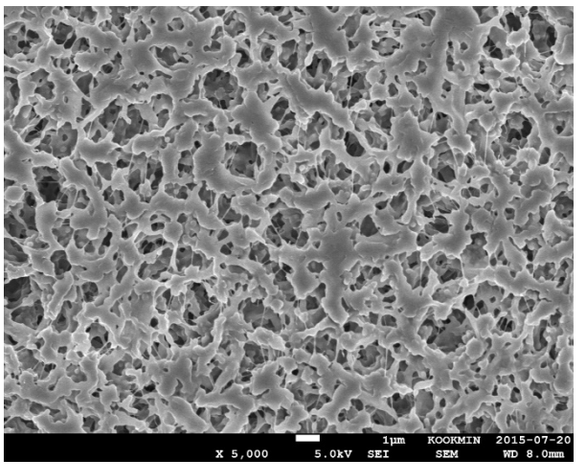

(a)

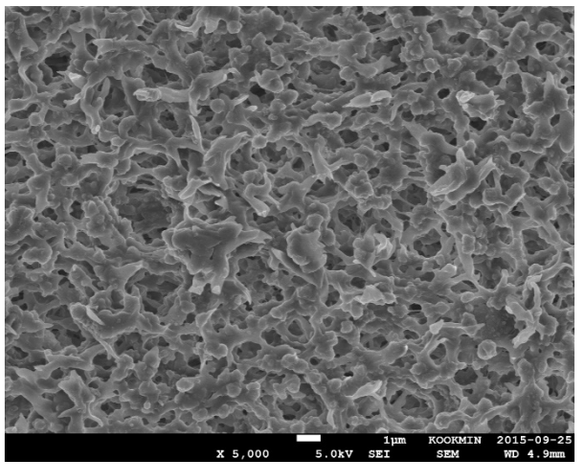

(b)

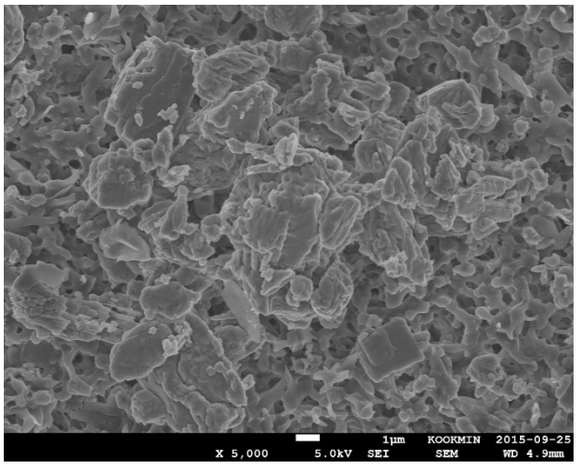

(c)

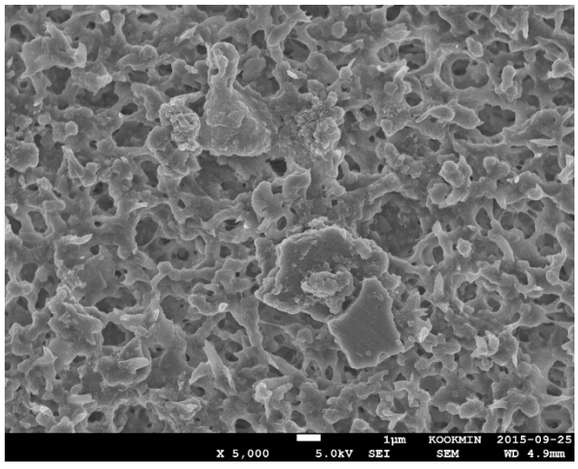

(d)

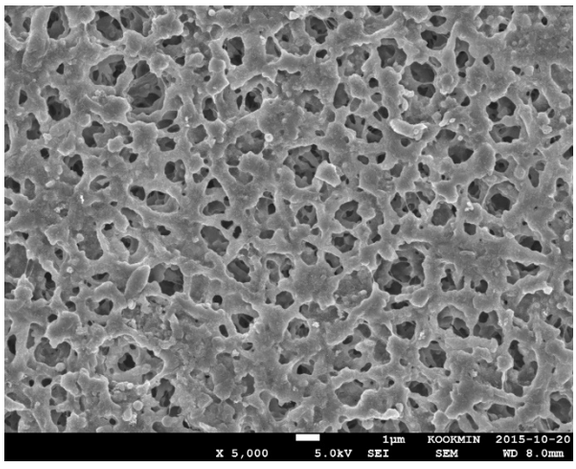

(e)

Fig. 4. Scanning electron microscopy (SEM) images of new membrane and membranes after fouling tests using single foulant solutions: (a) new membrane (control), (b) AL, (c) CA, (d) SM, and (e) TMA.

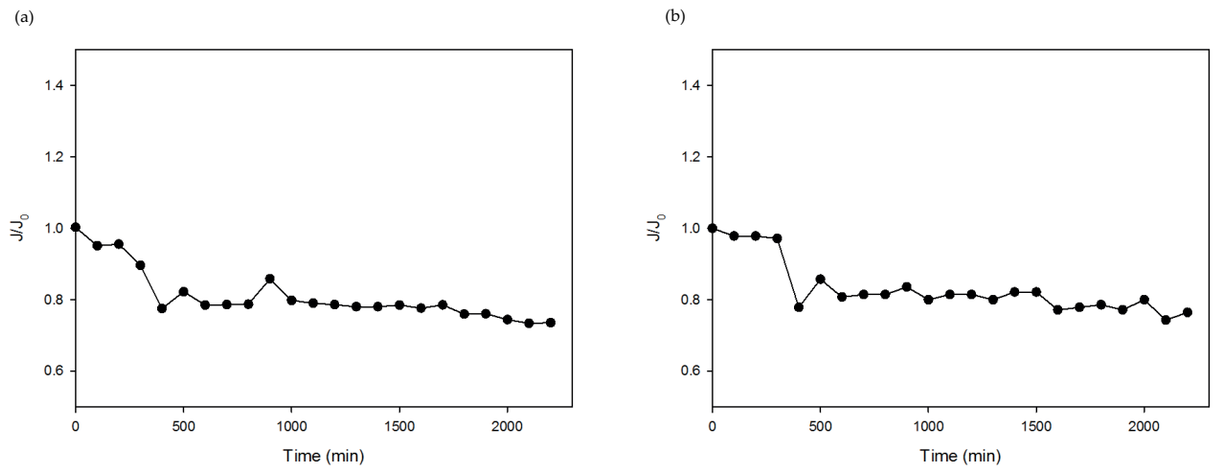

Fig. 5. Flux decline for MD of binary foulant solutions containing alginate and silica nanoparticles: (a) AL+SM and (b) AL+TMA.

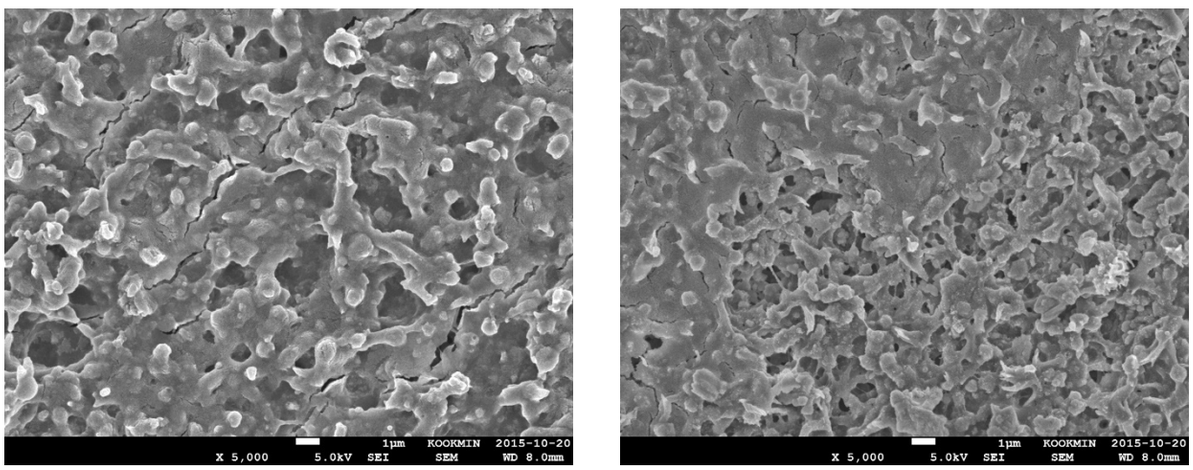

(a) (b)

Fig. 6. SEM images of membranes after fouling tests of binary foulant solutions: (a) AL+SM and (b) AL+TMA.

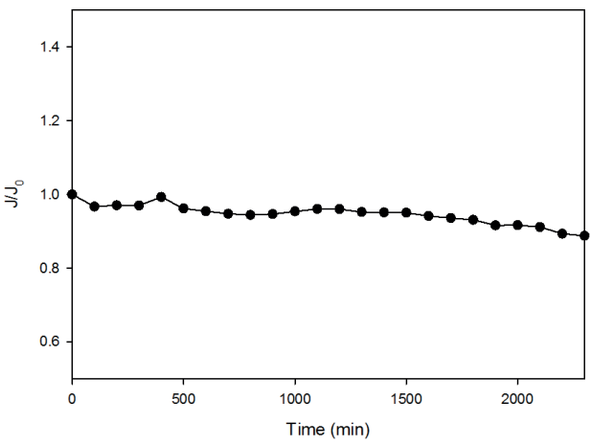

Fig. 7. Flux decline for MD of binary foulant solutions containing alginate and $CaCO_3$ (AL+CA).

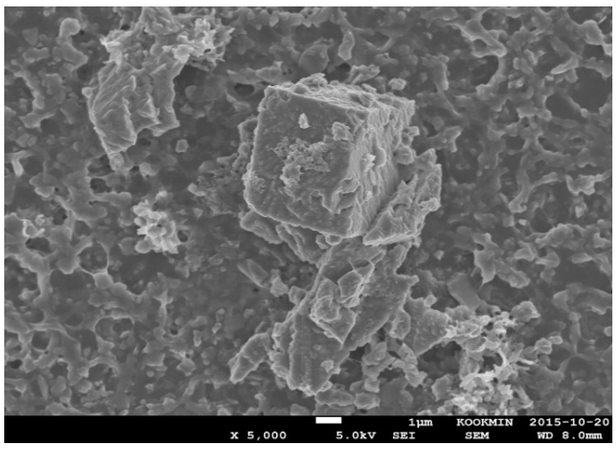

Fig. 8. SEM image of after fouling test of binary foulant solution (AL+CA).

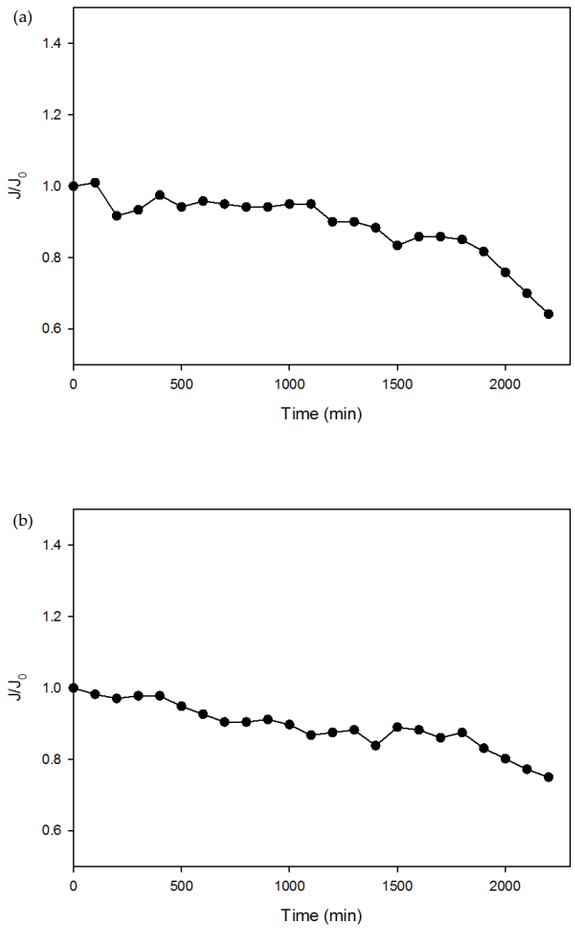

Fig. 9. Flux decline for MD of binary foulant solutions containing CaCO3 and silica Nanoparticles: (a) CA+SM and (b) CA+TMA.

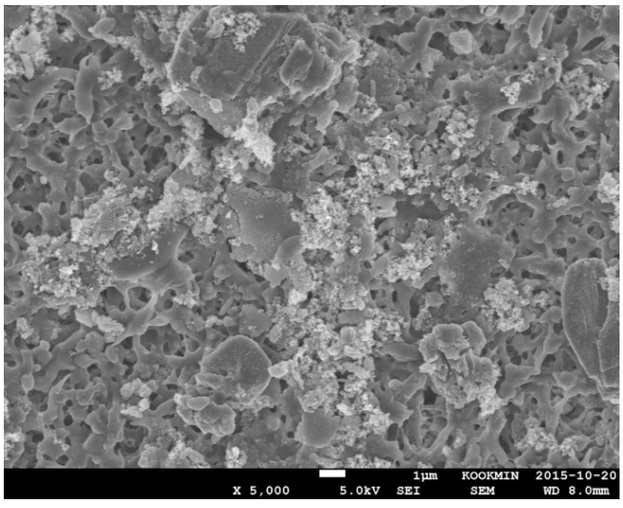

Fig. 10. SEM image of membranes after fouling test of binary foulant solution (CA+SM).

occur for $CaCO_3$ and alginate. The SEM image in Fig. 8 is similar to that for $CaCO_3$ in Fig. 4(c). Cubic-shaped crystal particles could be found in both cases. It appears that the fouling is mainly dominated by $CaCO_3$ and alginate does not cause additional fouling. Instead, alginate seems to slightly reduce the fouling propensity of $CaCO_3$ by changing the morphology of the deposition layer, leading to a slight increase in the J/J_0 value compared with that for CA foulant solution.

The mixtures of $CaCO_3$ and silica nanoparticles were also used to examine their fouling potential in MD process. The results are shown in Fig. 9. The J/J_0 value for CA+SM was 0.735 while those for AL and SM were 0.856 and 0.871, respectively. If these foulants individually caused flux decline, the J/J_0 value should be 0.727, which is similar to that for CA+SM. On the other hand, the J/J_0 value for CA+TMA was 0.75 while those for AL and TMA were 0.856 and 0.879, respectively. If these foulants individually caused flux decline, the J/J_0 value should be 0.735, which is only slightly lower than that for CA+TMA. Again, there seems to be no synergic effect by the combination of two different foulants. The morphology of the foulant layer is also different from those for $CaCO_3$ or silica. Foulant layer caused by $CaCO_3$ typically includes cube-shaped crystals as shown in Fig. 4(c). A cake layer was formed by the deposition of silica as depicted in Fig. 4(e). Nevertheless, not only the $CaCO_3$ crystals but also silica nanoparticles are observed from the SEM image in Fig. 10. It seems that two foulants individually cause flux decline without interactions.

3.3. Fouling caused by tertiary foulant solutions

The final case is with the tertiary foulant solutions including AL+CA+SM and AL+CA+TMA, implying not only organics (alignate) but also scale-forming ions ($CaCO_3$) and particles (SM or TMA) exist in these solutions. The results are shown in Fig. 11. Although three foulants are included in the feed solution, the fouling propensities are relatively low. The J/J_0 values for AL+CA+SM and AL+CA+TMA were 0.891 and 0.897, respectively. These values are even smaller than those for single foulants such as CaCO3, Ludox SM, and Ludox TMA. Instead of "positive" synergic effect, the tertiary foulant solution resulted in "negative synergic effect," which further reduces the fouling potentials for individual foulants.

This result can be explained by considering the possibility for competitive fouling by different foulants. If alginate can form the fouling layer first, it may prevent the scale formation by CaCO3 and also retard the fouling by silica deposition. In addition, the formation of floc-like structure may not be formed in the presence of $CaCO_3$ which may have an interaction with alginate. This mechanism is supported by the SEM image in Fig. 12. Unlike the case of fouling by $CaCO_3$, the foulant layer only contains insignificant amount of $CaCO_3$ crystals, implying that the scale formation on the membrane surface is prevented. Instead, the gel-like foulant layer is observed, which seems to be composed of alginate. Since the fouling potential by alginate is lower (0.956) than those by other foulants, the deposition of alginate can have beneficial effect on permeate flux.

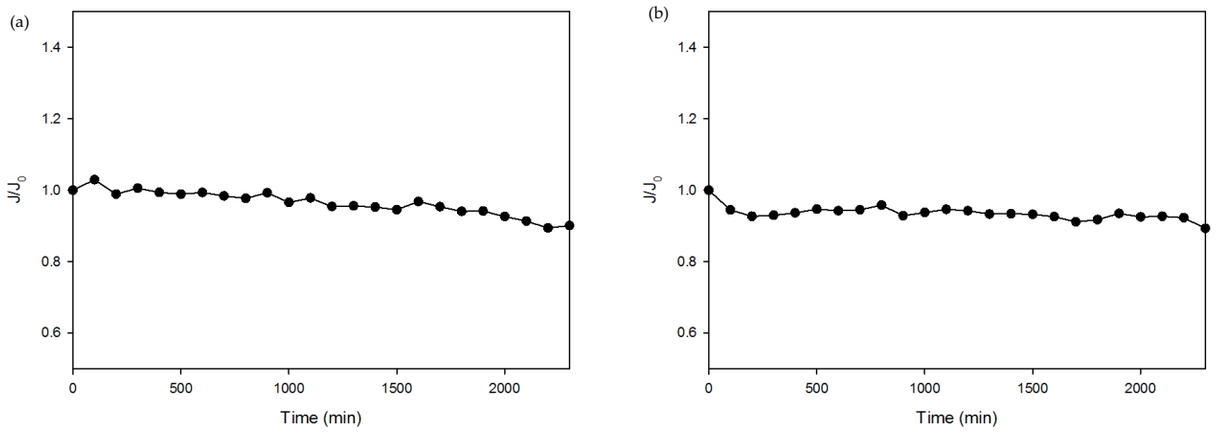

Fig. 11. Flux decline for MD of tertiary foulant solutions containing alginate, $CaCO_3$, and silica nanoparticles: (a) AL+CA+SM and (b) AL+CA+TMA.

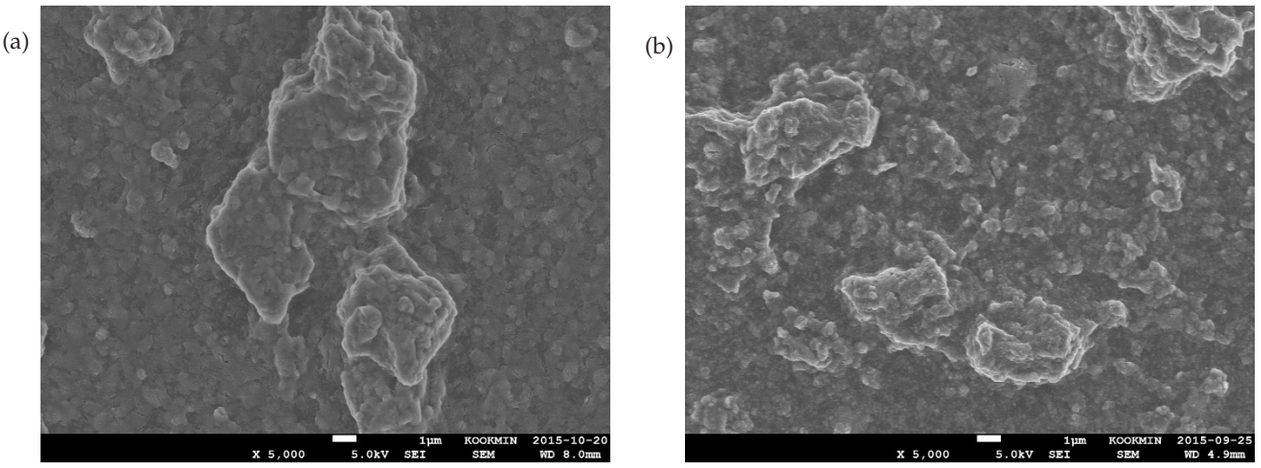

Fig. 12. SEM images of membranes after fouling tests using tertiary foulant solutions: (a) AL+CA+SM and (b) AL+CA+TMA.

3.4. Effect of fouling on LEP

In addition to flux decline due to membrane fouling, pore wetting is a serious problem in MD process and may occur together with the fouling. Accordingly, the effect of fouling on wetting of MD membranes was investigated by measuring LEP after the MD experiments using single or

Table 3
Comparison of liquid entry pressures (LEPs) for single foulant

Foulant	Control	Alginate (AL)	$CaCO_3$ (CA)	Ludox SM (SM)	Ludox TMA (TMA)
LEP (bar)	2.37	2.35	2.34	2.34	2.32

Table 4
Comparison of LEPs for multiple foulants

Foulants	AL+SM	AL+TMA	CA+SM	CA+TMA	AL+CA	AL+CA+SM	AL+CA+TMA
LEP (bar)	2.25	2.24	2.21	2.03	2.15	2.22	2.13

Table 5
Comparison of fouling potential ($1–J/J_0$) for single and binary foulant solutions

Foulant types	Organics	Colloids		Scale
Model foulants	AL	SM	TMA	CA
AL	0.044	0.27^+	0.233^+	0.09^-
SM		0.129		0.265
TMA			0.124	0.25
CA				0.144
AL+SM+CA	0.109			

$^+$ positive synergic effect.
$^-$ negative synergic effect.

multiple foulant solutions. Table 3 compares the LEP values for new membrane (control) with those for membranes after the fouling experiments using the single foulant solution. The LEP value for the new membrane is 2.37 bar while those after fouling by single foulants range from 2.32 (TMA) to 2.35 (AL). These values are only slightly lower than that for the new membrane, indicating that the wetting potentials for these foulants are not significant.

Using binary or tertiary foulant solutions, the LEP results were different from those with the single foulant solutions. As listed in Table 4, the LEP values were in the range between 2.03 and 2.25. The LEP value for CA+TMA was the lowest, and that for AL+SM was the highest. It is interesting to note that the wetting tendency is not always in accordance with the fouling propensity:

(1) Fouling potential ($1–J/J_0$): AL+SM (0.27) ≈ CA+SM (0.265) ≈ CA+TMA (0.25) > AL+TMA (0.233) > CA (0.144) > SM (0.129) ≈ TMA (0.124) > AL+CA+SM (0.109) ≈ AL+CA+TMA (0.103) > CA+AL (0.09) > AL (0.044)
(2) Wetting potential ($1\text{-LEP}/\text{LEP}_{control}$): CA+TMA (0.143) > AL+CA+TMA (0.101) > CA+AL (0.093) > CA+SM (0.068) ≈ AL+CA+SM (0.063) > AL+TMA (0.055) ≈ AL+SM (0.051) > TMA (0.021) > CA (0.013) ≈ SM (0.013) > AL (0.008)

The fouling potential was estimated by $1-J/J_0$, and the wetting potential was estimated by $1\text{-LEP}/\text{LEP}_{control}$. As listed above, the maximum fouling potential was found from the results of AL+SM, CA+SM, and CA+TMA while the maximum wetting potential was found from those of CA+TMA. In case of CA+TMA, the fouling potential and the wetting potential were the highest. However, in case of AL+SM and CA+SM, the fouling potentials were high, but the wetting potentials were moderate. On the other hand, the fouling potential and wetting potential were the lowest for AL.

Table 5 compares the fouling potential ($1-J/J_0$) for single and binary foulant solutions. The cells in the diagonal line represent the single foulant solutions and the other cells. Other cells represent the cases with the binary foulant solutions. This table helps to determine the interactions between two foulants. For example, the fouling potential by AL is 0.044, and that by SM is 0.129. On the other hand, the fouling potential by AL+SM is 0.27, which is larger than the sum of two fouling potentials by single foulants. Accordingly, it is concluded that AL and SM has a positive synergic effect that accelerates fouling by their interaction. In a similar manner, AL and TMA also has a positive synergic effect. However, the sum of two fouling potentials by AL and CA is larger than that by AL+CA, indicating that there is a negative synergic effect for AL+CA. According to the table, neither positive nor negative synergic effect appears to exist in case of SM+CA and TMA+CA. In addition, the tertiary foulant solution (AL+SM+CA) resulted in a negative syndetic effect (0.109) compared with the sum of three single foulant solutions (0.044 + 0.129 + 0.144 = 0.317).

Table 6 shows the summary of the comparison of wetting potential ($1\text{-LEP}/\text{LEP}_{control}$) for single and binary foulant solutions. Unlike the previous cases for fouling potential, positive synergic effects were found in all binary foulant solution. In addition, the tertiary foulant solution (AL+SM+CA) resulted in a positive syndetic effect (0.063) compared with the sum of three single foulant solutions (0.008 + 0.013 + 0.013 = 0.034). These results suggest that the behaviors of fouling and wetting are different for feed solutions containing different foulants. Although fouling is not severe, wetting may occur due to the interactions of two foulants. The results also imply that wetting potential by scale formation highly increases in the presence of other foulants.

Fig. 13 illustrates the schematics of proposed fouling mechanisms by binary foulant solutions. In case of SM+AL and TMA+AL, the adsorption of AL leads to an increased deposition of SM or TMA. In case of SM+CA, no interaction occurs, and thus the overall fouling potential is equal to the sum of individual fouling potentials. In case of CA+AL, the adsorption of AL can retard the formation of $CaCO_3$ crystals on the membrane surface, thereby reducing the fouling rate.

Table 6
Comparison of wetting potential ($1\text{-LEP}/\text{LEP}_{control}$) for single and binary foulant solutions

Foulant types	Organics	Colloids		Scale
Model foulants	AL	SM	TMA	CA
AL	0.008	0.051^+	0.021^+	0.093^+
SM		0.013		0.068^+
TMA			0.021	0.143^+
CA				0.013
AL+SM+CA	0.063			

$^+$ positive synergic effect.
$^-$ negative synergic effect.

Table 7
Comparison of fouling potential ($1-J/J_0$) and wetting potential ($1\text{-LEP}/\text{LEP}_{control}$) for binary and tertiary foulant solutions

Model foulants	AL+SM	SM+CA	CA+AL	AL+CA+SM
Fouling potential	0.27	0.265	0.09	0.109
Wetting potential	0.051	0.068	0.093	0.063

4. Conclusions

In this work, a comparative study of fouling propensity and wetting tendency for different foulants was performed using laboratory-scale MD experiments. The following conclusions can be drawn:

(1) The fouling potentials for single foulant solutions containing alginate or colloidal silica nanoparticles were not substantial. On the other hand, $CaCO_3$ resulted in noticeable fouling due to scale formation and particle deposition on the membrane surface.

(2) The fouling propensities for binary foulant solutions (AL+SM and AL+TMA) were higher than the sum of fouling propensities for individual foulants. This implies that a synergic effect exists by the interactions between alginate and silica particles.

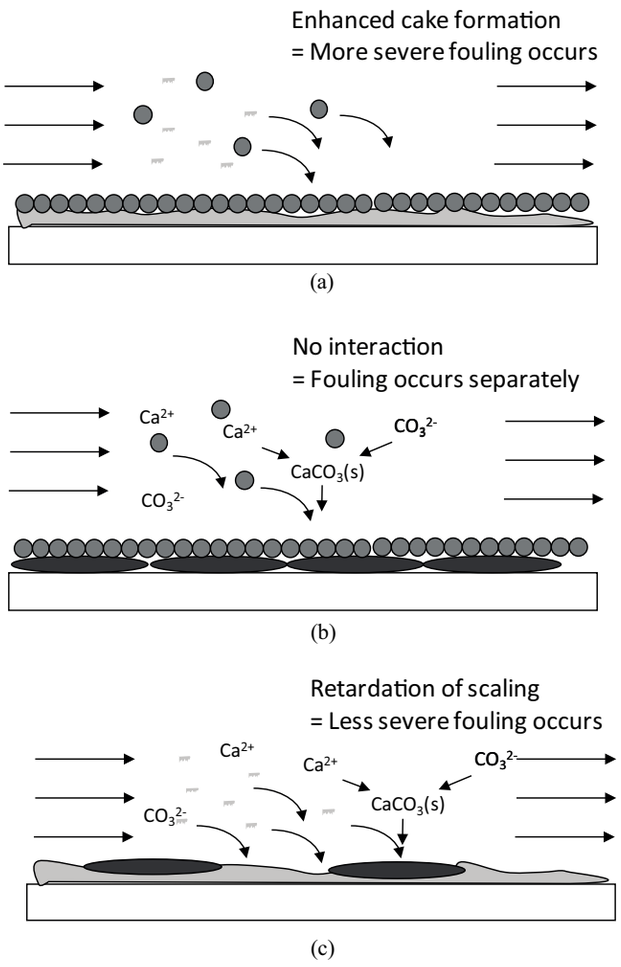

Fig. 13. Schematics of proposed fouling mechanisms by binary foulant solutions: (a) colloidal silica (SM or TMA) + organics (AL), (b) colloidal silica (SM or TMA) + scale ($CaCO_3$), and (c) scale ($CaCO_3$) + organics (AL).

(3) No synergic effect was observed in the case of $CaCO_3$ and silica (Ludox SM and TMA), indicating that the interaction between these two foulants are not significant. The fouling potential for the mixture of $CaCO_3$ and alginate (AL+CA) was lower than that for $CaCO_3$ (CA) and larger than that for alginate (AL).

(4) The tertiary foulant solutions containing alginate, $CaCO_3$, and silica (AL+CA+SM and AL+CA+TMA) result reduced fouling propensities compared with those for $CaCO_3$ (CA) and silica (SM or TMA). This result can be explained by considering the possibility for competitive fouling by different foulants and confirmed by the SEM analysis.

(5) The wetting potential measured by LEP value was not significant for single foulants but higher for binary or tertiary foulants. Moreover, the wetting tendency is not always in accordance with the fouling propensity.

Acknowledgment

This research was supported by a grant (code 15IFIP-B065893-03) from Industrial Facilities & Infrastructure Research Program funded by Ministry of Land, Infrastructure and Transport of Korean government and also by Korea Ministry of Environment as Global Top Project (Project No.: GT-14-B-01-003-0).

References

[1] P.S. Goh, T. Matsuura, A.F. Ismail, N. Hilal, Recent trends in membranes and membrane processes for desalination, Desalination, 391 (2016) 43–60.
[2] V.G. Gude, Energy storage for desalination processes powered by renewable energy and waste heat sources. Appl. Energy, 137 (2015) 877–898.
[3] V.G. Gude, Desalination and sustainability – An appraisal and current perspective. Water Res., 89 (2016) 87–106.
[4] S.S. Shenvi, A.M. Isloor, A.F. Ismail, A review on RO membrane technology: developments and challenges, Desalination, 368 (2015) 10–26.
[5] N. Ghaffour, J. Bundschuh, H. Mahmoudi, M.F.A. Goosen, Renewable energy-driven desalination technologies: a comprehensive review on challenges and potential applications of integrated systems, Desalination, 356 (2015) 94–114.
[6] A. Subramani, J.G. Jacangelo, Emerging desalination technologies for water treatment: a critical review, Water Res., 75 (2015) 164–187.
[7] F. Suárez, J.A. Ruskowitz, S.W. Tyler, A.E. Childress, Renewable water: direct contact membrane distillation coupled with solar ponds, Appl. Energy, 158 (2015) 532–539.
[8] Y. Zhang, Y. Peng, S. Ji, Z. Li, P. Chen, Review of thermal efficiency and heat recycling in membrane distillation processes. Desalination, 367 (2015) 223–239.
[9] E. Drioli, A. Ali, F. Macedonio, Membrane distillation: recent developments and perspectives, Desalination, 356 (2014) 56–84.
[10] A. Alkhudhiri, N. Darwish, N. Hilal, Membrane distillation: a comprehensive review, Desalination, 287 (2012) 2–18.
[11] S. Yarlagadda, V.G. Gude, L.M. Camacho, S. Pinappu, and S. Deng, Potable water recovery from As, U, and F contaminated ground waters by direct contact membrane distillation process. J. Hazard. Mater., 192 (2011) 1388–1394.
[12] M. Peter-Varbanets, C. Zurbrügg, C. Swartz, W. Pronk, Decentralized systems for potable water and the potential of membrane technology, Water Res., 43 (2009) 245–265.
[13] A. Hausmann, P. Sanciolo, T. Vasiljevic, U. Kulozik, M. Duke, Performance assessment of membrane distillation for skim milk and whey processing, J. Dairy Sci., 97 (2014) 56–71.
[14] W. Kujawski, A. Sobolewska, K. Jarzynka, C. Güell, M. Ferrando, J. Warczok, Application of osmotic membrane distillation process in red grape juice concentration, J. Food Eng., 116 (2013) 801–808.
[15] Ramato A. Tufa, E. Curcio, E. Brauns, W. van Baak, E. Fontananova, G. Di Profio, Membrane distillation and reverse electrodialysis for near-zero liquid discharge and low energy seawater desalination, J. Membr. Sci., 496 (2015) 325–333.
[16] L.D. Tijing, Y.C. Woo, J.S. Choi, S. Lee, S.H. Kim, H.K. Shon, Fouling and its control in membrane distillation—a review. J. Membr. Sci., 475 (2015) 215–244.
[17] D.M. Warsinger, J. Swaminathan, E. Guillen-Burrieza, H.A. Arafat, J.H. Lienhard V, Scaling and fouling in membrane distillation for desalination applications: a review, Desalination, 356 (2015) 294–313.
[18] J. Ge, Y. Peng, Z. Li, P. Chen, S. Wang, Membrane fouling and wetting in a DCMD process for RO brine concentration, Desalination, 344 (2014) 97–107.

[19] S. Goh, J. Zhang, Y. Liu, A.G. Fane, Fouling and wetting in membrane distillation (MD) and MD-bioreactor (MDBR) for wastewater reclamation, Desalination, 323 (2013) 39–47.
[20] E. Guillen-Burrieza, A. Servi, B.S. Lalia, H.A. Arafat, Membrane structure and surface morphology impact on the wetting of MD membranes, J. Membr. Sci., 483 (2015) 94–103.
[21] J.A. Bush, J. Vanneste, T.Y. Cath, Membrane distillation for concentration of hypersaline brines from the Great Salt Lake: effects of scaling and fouling on performance, efficiency, and salt rejection, Sep. Purif. Technol., 170 (2016) 78–91.
[22] J.A. Sanmartino, M. Khayet, M.C. García-Payo, H. El Bakouri, A. Riaza, Desalination and concentration of saline aqueous solutions up to supersaturation by air gap membrane distillation and crystallization fouling, Desalination, 393 (2016) 39–51.
[23] Y.Z. Tan, J.W. Chew, W.B. Krantz, Effect of humic-acid fouling on membrane distillation, J. Membr. Sci., 504 (2016) 263–273.
[24] W. Zhong, H. Li, Y. Ye, V. Chen, Evaluation of silica fouling for coal seam gas produced water in a submerged vacuum membrane distillation system, Desalination, 393 (2016) 52–64.